Journal of Magnetism and Magnetic Materials 500 (2020) 166386

Contents lists available at ScienceDirect

Journal of Magnetism and Magnetic Materials

journal homepage: www.elsevier.com/locate/jmmm

Research articles

The influence of cation ordering and oxygen nonstoichiometry on magnetic properties of Sr_2FeMoO_{6-x} around Curie temperature

Nikolay Kalanda[a,*], Marta Yarmolich[a], Alexander Petrov[a], Igor Raevski[b], Stanislav Kubrin[b], Svetlana Raevskaya[b], Ivan Bobrikov[c], Andrei Lazavenka[d], Dong-Hyun Kim[e]

[a] Scientific-Practical Materials Research Centre of NAS of Belarus, P.Brovka Str. 19, 220072 Minsk, Belarus
[b] Physics Research Institute and Faculty of Physics, Southern Federal University, R.Zorghe Str. 5, 344090 Rostov-on-Don, Russia
[c] I.M. Frank Laboratory of Neutron Physics, Joint Institute for Nuclear Research, 141980 Dubna, Russia
[d] Belarusian State University of Informatics and Radioelectronics, P.Brovka Str. 6, 220013 Minsk, Belarus
[e] Department of Physics, Chungbuk National University, 410 Sungbong-ro, Gaesin-dong, 361-763 Cheongju, Chungbuk, South Korea

ARTICLE INFO

Keywords:
Strontium ferromolybdate
Oxygen nonstoichiometry
Superstructural ordering
Mössbauer spectroscopy
Magnetization
Exchange interactions

ABSTRACT

Sr_2FeMoO_{6-x} polycrystalline samples with different oxygen content $(6-x)$ and various degrees of superstructural ordering of Fe/Mo cations (P) were obtained by the solid-phase method from the $SrFeO_{2.52}$ and $SrMoO_4$ precursors. From the investigation on the influence of oxygen non-stoichiometry and the P parameter on the magnetic properties of Sr_2FeMoO_{6-x}, it was found that with an increase in P and a decrease in the $(6-x)$ value from 5.99 to 5.94, an increase in the magnetization values is observed in the temperature range 77–600 K. For all the Sr_2FeMoO_{6-x} samples there is a tendency that P value rises with increasing x, where, accordingly, the volume fraction of regions in which there are no anti-structural defects increases as well. This is also indicated by Mössbauer spectroscopy data, confirming an increase in the area of the S1 sextet corresponding to Fe ions in highly ordered regions and a decrease in the area of the S2 sextet associated with disordered regions. Using the temperature scanning method, the temperatures of the onset and completion of the transition from the paramagnetic to the ferrimagnetic state and, correspondingly, the blurring width of the transition have been estimated. It turned out that with decreasing P, the blurring of the transition increases, which is associated with an increase in the concentration of anti-structural defects.

1. Introduction

The strontium ferromolybdate Sr_2FeMoO_{6-x} with a double perovskite structure is one of prospective materials for applications in the microelectronic industry such as magnetic random access memory (MRAM), magnetic reading heads for hard disk drives, highly-sensitive magnetic field sensors and fuel cell electrodes [1–3]. For these applications, structurally perfect Sr_2FeMoO_{6-x} samples with high Curie temperatures, saturation magnetization, large degree of the Fe/Mo cations superstructural ordering as well as the high spin polarization of the delocalized electrons are required [4–7].

Thus, a technology for fabricating high-grade structurally perfect Sr_2FeMoO_{6-x} samples with reproducible magnetic and electrical transport properties is of utmost importance. One of the most important conditions of the existence of the maximal spin-polarization degree in the strontium ferromolybdate is the superstructural ordering of Fe and Mo cations, located at the centers of the octahedra, while there are oxygen anions O(1) and O(2) at the vertices [8]. In an actual crystal structure, due to the presence of various point defects, especially the anti-structural ones ($[Mo]_{Fe}$ and $[Fe]_{Mo}$), as well as the anionic vacancies V_O, the crystal structure becomes distorted. It leads to the redistribution of the electronic density and a formation of iron cations, Fe^{2+}, $3d^6\{S = 2\}$ and molybdenum cations, Mo^{6+}, $4d^0\{S = 0\}$. Diamagnetic cations $Mo^{6+}(4d^0)$ do not take part in the exchange interactions, and only negative exchange interactions are possible between the Fe^{2+} $(3d^6)$ or Fe^{3+} $(3d^5)$ ions, which leads to a formation of the antiferromagnetic ordering of their magnetic moments.

Physical-chemical properties of the Sr_2FeMoO_{6-x} considerably depend on the oxygen stoichiometry, which influence the degree of superstructural ordering of the iron and molybdenum cations, orbital, charge and spin degrees of freedom and correspondingly on the electronic exchange between $Fe^{3+}$and Mo^{5+} [9–11]. The presence of oxygen ion or their vacancies on the Sr_2FeMoO_{6-x} grains surface promotes a modification of the charge electronic density on the grain

* Corresponding author.
E-mail address: kalanda@physics.by (N. Kalanda).

https://doi.org/10.1016/j.jmmm.2019.166386
Received 9 October 2019; Received in revised form 12 December 2019; Accepted 31 December 2019
Available online 02 January 2020

boundaries and in the sub-surface area of the grain. With that, oxidation-recovery processes can reversibly change the oxygen stoichiometry both in the grains and in the grain boundaries. Therefore, magnetic and galvanomagnetic properties can be altered as well [12–14]. This evidences a high sensitivity of the Sr_2FeMoO_{6-x} compound to the parameters of the synthesis, substantially depending on the oxygen non-stoichiometry and the iron/molybdenum cation superstructural ordering, which might be different from one sample to another.

Therefore, the strontium ferromolybdate samples with well-controlled oxygen content with reproducible physical characteristics should be studied for a correct understanding of the processes and fundamental mechanisms. In this work, we report our systematic investigations on the effect of cation ordering and oxygen non-stoichiometry for the strontium ferromolybdate with a special importance in the details of the local atomic order in the magnetic grains. Our investigation reveals the regularities in the atoms placement on a scale compared with the interatomic one, which is interrelated with the oxygen vacancies concentration and the superstructural ordering of the Fe/Mo cations.

2. Material and methods

Sr_2FeMoO_{6-x} polycrystalline samples were synthesized by the solid-phase technique from the $SrFeO_{2.52}$ and $SrMoO_4$ precursors. The precursors were prepared by the conventional ceramic technique from MoO_3, Fe_2O_3 and $SrCO_3$. Milling and compounding of the stoichiometric mixture of the initial reagents have been carried out in the vibromill in alcohol during 3 h. The obtained mixtures were dried at 350 K and pressed into pellets. In the process of the $SrFeO_{3-x}$ and $SrMoO_4$ precursors synthesis, the preliminary annealing was carried out on air at 970 K and 1070 K during 20 and 40 h, respectively. For the increase of the batch homogeneity, a secondary milling has been applied. The final synthesis for the $SrFeO_{3-x}$ compound was realized at 1470 K during 20 h in the argon flow, and the synthesis for the $SrMoO_4$ compound was realized at 1470 K during 40 h at $p(O_2) = 0.21 \times 10^5$ Pa with a subsequent tempering at the room temperature. The oxygen content in the $SrFeO_{3-x}$ compound was determined by its weighing, before and after its complete recovery in the hydrogen flow at 1373 K during 20 h to the SrO simple oxide and Fe metal. It was determined that the strontium ferrite has a composition $SrFeO_{2.52}$.

A synthesis of the strontium ferromolybdate was carried out in pellets with diameter of 10 mm and thickness of 4–5 mm, pressed from the initial reagents $SrFeO_{2.52}$ and $SrMoO_4$ in the stoichiometric ratio. Pellets was annealed in a flow of the 5% H_2/Ar gas mixture at 1420 K during 5 h with a subsequent tempering at room temperature. The oxygen content in the Sr_2FeMoO_{6-x} compound was determined by the weighing before and after the complete recovery in the hydrogen flow at 1373 K during 20 h to the SrO simple oxide together with the Fe and Mo metals.

Samples with a various oxygen content and a different superstructural ordering of Fe/Mo cations were obtained by means of the annealing of Sr_2FeMoO_{6-x} at 1420 K in the 5% H_2/Ar gas mixture flow during 20 h – *A*-1 ($Sr_2FeMoO_{5,97}$, $P = 76\%$), during 50 h – *A*-2 ($Sr_2FeMoO_{5,94}$, $P = 86\%$), and 90 h – *A*-3 ($Sr_2FeMoO_{5,94}$, $P = 93\%$). A presence of the (1 0 1) reflex indicates the formation of Fe/Mo cations superstructural ordering in the Sr_2FeMoO_{6-x} unit cell (Fig. 1).

Phase composition and the crystal lattice parameters were determined using the ICSD–PDF2 (Release 2000) database and PowderCell, FullProf software by the Rietveld technique on the base of the XRD data. The XRD patterns were taken at room temperature with the rate 60°/h in the angular range 10–90° on the DRON-3 setup in the CuK_α emission. The degree of iron and molybdenum cations superstructural ordering (P) has been calculated by the formula $P = (2 \cdot SOF - 1) \cdot 100\%$, where SOF is the factor of the population of positions calculated on the base of the XRD data.

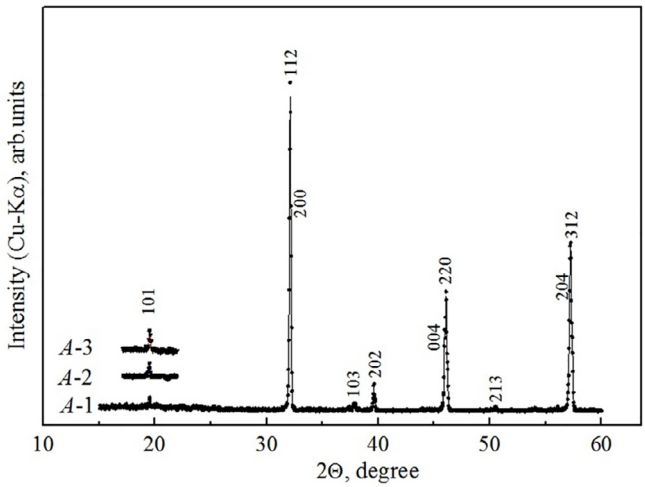

Fig. 1. XRD patterns of the *A*-1, *A*-2 and *A*-3 samples.

Mössbauer spectra were measured by means of the MS1104Em spectrometer. ^{57}Co in the Rh matrix has been used as a source of the γ-quanta. The Mössbauer spectra were measured in the constant accelerations mode in the moving source geometry; the rate value was measured by the law of triangle. For the cooling process the samples were placed in the CCS-850 (Janisinc) helium cryostat cavity. Heating of the samples has been carried out in the furnace with the air atmosphere. The model identification of spectra was carried out by means of the SpectrRelax program [15]. Isomer shifts were calculated relative to the metallic α-Fe.

The Curie temperature has been determined in the process of investigations of the Sr_2FeMoO_{6-x} samples magnetization temperature dependences by the ponderomotive method in the temperature range 77–600 K in the external magnetic field 0.86 T by means of the "Liquid Helium Free High Field Measurement System" setup by the Cryogenic Ltd., containing the closed cycle refrigerator.

3. Results and discussion

The effect of oxygen nonstoichiometry and the Fe/Mo cations superstructural ordering degree on the magnetic properties has been explored. Firstly, with the increase of P from 76 (*A*-1) to 93% (*A*-3), the oxygen index ($6-x$) decreases from 5.99 to 5.94, where the magnetization $M(T)$ measured in the magnetic field 0.86 T is observed to increase in the temperature range 77–600 K. At 77 K, $M(A\text{-}1)_{77K} = 26.41$, $M(A\text{-}2)_{77K} = 32.36$ and $M(A\text{-}3)_{77K} = 42.66$ A m^2 kg^{-1}.

The transition from the paramagnetic to the ferrimagnetic state in these samples is diffused. Measurements of the temperature dependences of the magnetization has made it possible to determine the starting temperature of this transition (T_C) at the cooling process, which corresponds to the crossing of tangent lines plotted to the $M(T)$ curves. Determined T_C values are found to increase from 422, 428, to 437 K for the samples with $P = 76$, 86 and 93%, respectively (Fig. 2).

This is explainable based on the fact that the Fe_{Mo} and Mo_{Fe} anti-structural defects concentration $n = (100-P)/2 = 3.5\%$, which is considered to be nearly absent in the case of $P = 93\%$ and $(6-x) = 5.94$. According to the neutron diffractometry data, the ordered double perovskite lattice is observed with alternating FeO_6 and MoO_6 octahedrons along all the three crystallographic axis [16]. A decrease of the P value with the increase of the $(6-x)$ value leads to the appearance of Fe_{Mo} and Mo_{Fe} anti-structural defects, where the Fe cations occupy the Mo sites and vice versa. Besides, the anti-structural defects result in a decrease of the T_C values as well as magnetization in the overall temperature range. Monotonic decrease of T_C with the lowering of P value might be also correlated with an increase of the

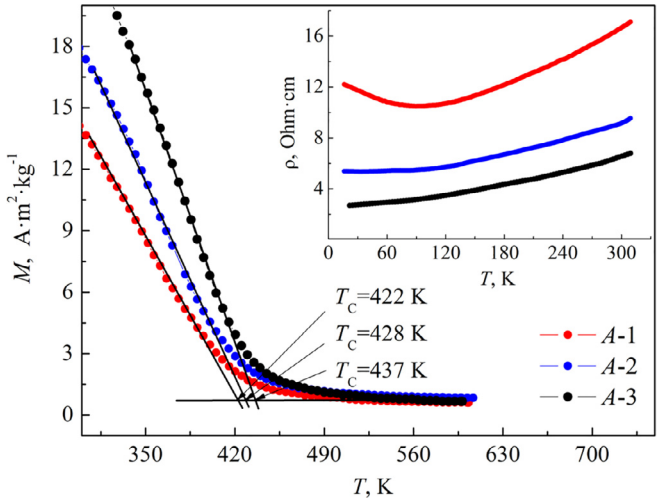

Fig. 2. Temperature dependences of the *A*-1, *A*-2 and *A*-3 samples magnetization, measured at the magnetic field of 0.86 T. Insert: temperature dependences of the electrical resistivity of the samples.

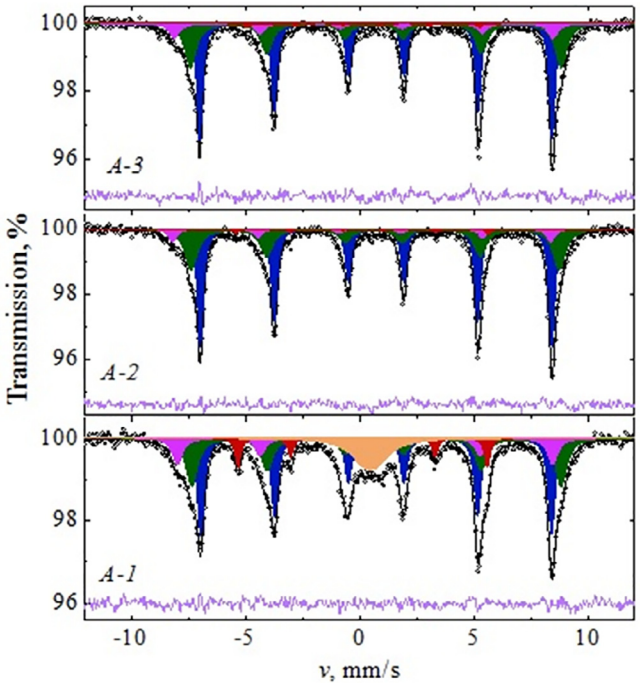

Fig. 3. Mössbauer spectra of the Sr_2FeMoO_{6-x} samples measured at 14 K (the blue sextet is Fe^{3+} in the ordered clusters; the green sextet is Fe^{3+} in the disordered clusters; the purple sextet is Fe^{3+}in the defect clusters; the red doublet is the metallic Fe; the orange doublet is the impurity phase). (For interpretation of the references to colour in this figure legend, the reader is referred to the web version of this article.)

electrical resistivity due to a drop down of the density of states at the Fermi level (Table 1).

The Mössbauer spectroscopy data indicate the influence of the oxygen vacancies and the *P* value on the change of the free charge carrier concentration on the Fermi level. The spectra measured at 14 K, are the superposition of the four Zeeman sextets (Fig. 3). The S1, S2 and S3 sextets are related to the perovskite phase.

The S1 sextet isomer shift value ($\delta_1 \approx 0.71$ mm/s), which is larger than the isomer shift values observed for Fe^{3+}cations in perovskites at low temperatures (Table 2). As a rule, δ values at low temperatures for Fe^{3+} in perovskites are in the range 0.49–0.55 mm/s [16–20]. With that, the δ_1 value of the S1 sextet is considerably lower than the values for Fe^{2+} in the oxygen octahedrons (≈1.2–1.8 mm/s) [18].

Therefore, the δ_1 value corresponds to the mixed valent state $Fe^{2+/3+}$. According to the perovskite band structure, electrons of the $Fe^{3+}3d^5$ cations with spins ↑ are placed in the valence band lower than the Fermi level on the $(t_{2g})\uparrow$and $(e_g)\uparrow$orbitals, and electrons of the $Mo^{5+}4d^1$ cations with spins ↓ are placed in the conduction band on the $(t_{2g})\downarrow$ orbitals (Fig. 4). According to the electronic structure calculations [7], an overlap of the (t_{2g}) electronic orbitals of the Mo *d*-level and the (t_{2g}) electronic orbitals of the Fe *d*-level takes place in the Sr_2FeMoO_{6-x} compound. The overlap leads to the Mo d^1 electron shift to the position of iron, whereupon the Fe^{3+} valent state is lowered to the values $Fe^{2+/3+}$ [21–23].

Value of the δ_2 of S_2 sextet is even larger than the values for Fe^{3+}, and it is lower than δ_1. A difference of the δ_1 and δ_2 values is possibly caused by a distinction in the cation environment of the Fe ions. Obviously, a larger value of δ_1 is caused by the fact that predominantly Mo cations are the nearest neighbors of the corresponding Fe ions, while the Fe ions, corresponding to the S2 sextet with δ_2, are surrounded by a smaller quantity of the Mo cations. Therefore, the S1 sextet probably corresponds to the $Fe^{2+/3+}$ions in highly-ordered areas and the S2 sextet corresponds to the $Fe^{2+/3+}$ ions in disordered areas. Moreover, an overlap of the Mo_{t2g} band and the low-spin Fet_{2g} band, leads to the decrease of the complete magnetic moments of the Fe ions from 5 μ_B to 4.4 μ_B [7]. Consequently, the value of the hyperfine magnetic field *H* intensity for the Fe ions in the highly-ordered areas should be lower than the corresponding values, usually observed for the high-spin Fe^{3+}ions in the oxygen octahedrons at low temperatures (500 kOe and higher) [18–20]. The S1 and S2 sextets of the Mössbauer spectra of the $Sr_2FeMoO_{6-\delta}$ samples possess $H_1 \approx 477$ kOe and $H_2 = 500$ kOe at 14 K (Table 2). The outlined values confirm the assumption that the appearance of the S1 and S2 sextets are caused by Fe ions in the ordered and disordered areas, respectively.

Since the Sr_2FeMoO_{6-x} samples differ by the ordering degree of the *B*-sublattice cations, as far as the ordering degree is lowered, the decrease of the S1 sextet area is observed, with a simultaneous increase of the S2 sextet area. The area value *A* of the Mössbauer spectra components is proportional to the Fe ions concentration in the corresponding phases. Changes of the spectra areas with the lowering of the ordering degree are in good agreement with the XRD investigations data (Fig. 1). With that, the absolute values of ordered and disordered phases concentrations obtained by means of the Mössbauer spectroscopy data, are lower than the values obtained from the analysis of the XRD patterns. This is possibly concerned with the fact that the disordered phase is formed in the areas divided by the ordered phase. As a result, part of iron ions of the ordered phase, placed on the boundaries with a disordered phase, forms a signal corresponding to the disordered phase.

The δ_3 value of the S3 sextet corresponds to Fe^{3+}ions with the

Table 1
Fe/Mo cations superstructural ordering degree (*P*), oxygen nonstoichiometry $(6-x)$, resistivity at 300 K (ρ_{300K}), Curie temperature (T_C), and the magnetization at 300 K at $B = 0.86$ T for the *A*-1, *A*-2 and *A*-3 samples.

Sample	$P \pm 1$, %	$(6-x) \pm 0.01$	$\rho_{300K} \pm 0.01$, Ohm cm	$T_C \pm 1$, K	$M_{300K} \pm 0.01$, A m^2 kg^{-1}
A-1	76	5.97	16.89	422	13.73
A-2	86	5.94	9.4	428	17.36
A-3	93	5.94	6.73	437	22.91

Table 2
Parameters of the Mössbauer spectra of the Sr_2FeMoO_{6-x} samples, measured at 14 K.

Sample	Component	δ ± 0.01, mm/s	δ*, mm/s	ε/Δ ± 0.01, mm/s	H ± 1, kOe	A ± 1, %	G ± 0.01, mm/s	χ^2
A-3	S1	0.71	0.47–0.55 [18]	0.00	477	52	0.30	1.415
	S2	0.65	0.54 [19]	0.04	502	36	0.60	
	S3	0.33	0.51 [20]	−0.16	524	10	0.52	
	S4	0.12		0.03	315	2	0.29	
A-2	S1	0.71		0.00	476	55	0.31	1.333
	S2	0.63		0.04	498	36	0.65	
	S3	0.26		−0.18	527	7	0.42	
	S4	0.12		−0.02	342	2	0.29	
A-1	S1	0.71		0.00	475	37	0.34	1.375
	S2	0.67		0.05	500	28	0.61	
	S3	0.33		−0.11	514	13	0.53	
	S4	0.13		−0.01	334	9	0.29	
	D1	0.46		0.61		13	1.46	

where δ is the isomer shift; δ* is isomer shift value taken from the literature, ε is the quadrupole shift; Δ is the quadrupole splitting; H is the hyperfine magnetic field on the ^{57}Fe nuclei; A is the area of the spectrum components; G is the width of the lines; χ^2 is the Pearson criterion

coordination number of 4–5 [17,24], which is caused by the presence of the oxygen deficiency in the investigated samples. The values of isomer shift and hyperfine magnetic field (H) of the S4 sextet are close to the values observed for the Fe^{3+} ions, placed in clusters in the state being close to the metallic one [17,18]. Results of the small-angle neutron scattering investigations also indicate the presence of magnetically-inhomogeneous state in the samples with magnetic regions having different magnetic nature [25]. The paramagnetic doublet, which is presumably caused by the presence of the superparamagnetic state in the part of Sr_2FeMoO_{6-x} grains, is observed for the *A*-1 sample.

Therefore, it flows from the above stated information, that a tendency in the *A*-1, 2, 3 samples is observed, when with the increase of oxygen nonstoichiometry and Fe/Mo cations superstructural ordering, the volumetric fraction of the defectless areas (areas with the ordered placement of iron and molybdenum cations) is rising. This circumstance indicates that the spin-polarized charge carriers on the Fermi level play an important role in the exchange interactions, which agrees with conclusions from previous reports [26,27]. Let us consider possible types of exchange interactions for the description of the obtained results.

According to the Goodenough – Kanamori – Anderson rule [28], at the overlap of the occupied and the empty electronic orbital of metal through a ligand, this exchange is the ferromagnetic one without the spin-flip at the overlap angle in the metal-ligand-metal chain, equal to ~80°. On this concern, one could suppose that exchange interactions between cations with different valencies in the Sr_2FeMoO_{6-x} compound through the oxygen anion ($Fe^{3+} - O^{2-} - Mo^{5+}$) are realized through the double exchange Zener mechanism. In this case, 100% degree of the spin polarization of electrons being in the conduction band is preserved. At that, the double exchange process takes place between the $Fe4d^0(t_{2g})\downarrow$ and $Mo4d^1(t_{2g})\downarrow$ orbitals, as the iron electronic levels are empty, and one electron is placed on the molybdenum level. This electron can hop between the orbitals (Fig. 5).

One could suppose that the exchange interaction between the magnetic cations of iron and molybdenum takes place through the excited O^{2-} anions, in the same way as in manganites. Upon the overlap of the wave functions of the nonmagnetic anions 2*p* orbitals and the iron magnetic cations 4*d* orbitals, a finite probability of the transition of 2*p* electron to the 4*d* electronic orbital exists. The O^{1-} oxygen anion passes to the excited state and it becomes the magnetic one with spin S = ½. As a result of the exchange interactions of the magnetic anion with the molybdenum cation, the electron is hopping from the 4*d* electronic orbital of molybdenum to the 2*p* orbital of anion (Fig. 5).

Therefore, it is supposed on the base of the above argument, that the exchange interaction between iron and molybdenum cations observed in the double perovskite might take place in frames of the Zener mechanism, as in the case of manganites [29–31]. Nevertheless, it should be mentioned that according to the neutron diffraction data, the Mo $4d^1$ cations possess a very small magnetic moment about μ(Mo) ~ 0.0(1)–0.42(6) μ_B [32,33], which indicates a delocalized character of electrons with spins ↓, placed on the Mo $(t_{2g})\downarrow$ electronic orbitals. Moreover, as we have shown above, the distance between the Fe cations in the Sr_2FeMoO_{6-x} crystal structure is ~7.9 Å, whereas the distance between Mn cations in manganites is ~3.5 Å. At the same time, this factor did not preclude the double perovskite from having the higher T_C values, than those for the manganites, implying the presence

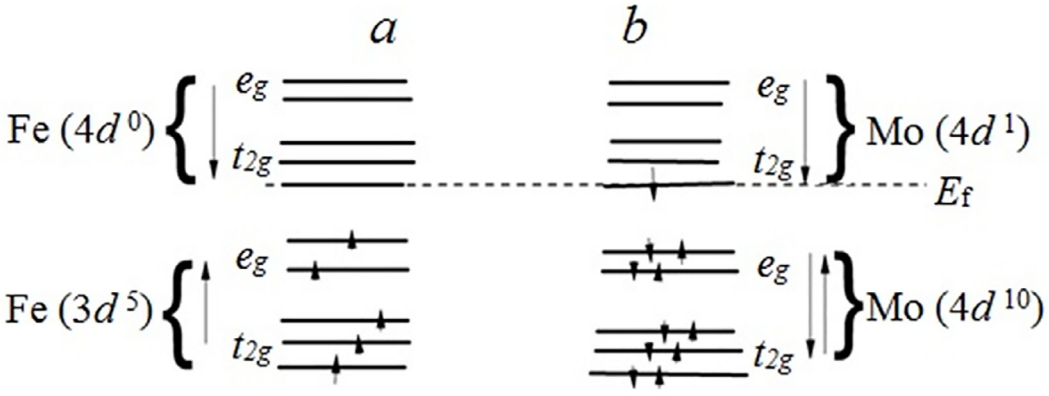

Fig. 4. Schematic image of the electrons distribution on the energy levels of iron ($Fe^{3+}3d^5$) and molybdenum ($Mo^{5+}4d^1$) in the Sr_2FeMoO_{6-x} compound at the absence of the anti-structural defects. A position of the Fermi level is indicated by the dashed line. (a) Iron energy levels; (b) molybdenum energy levels.

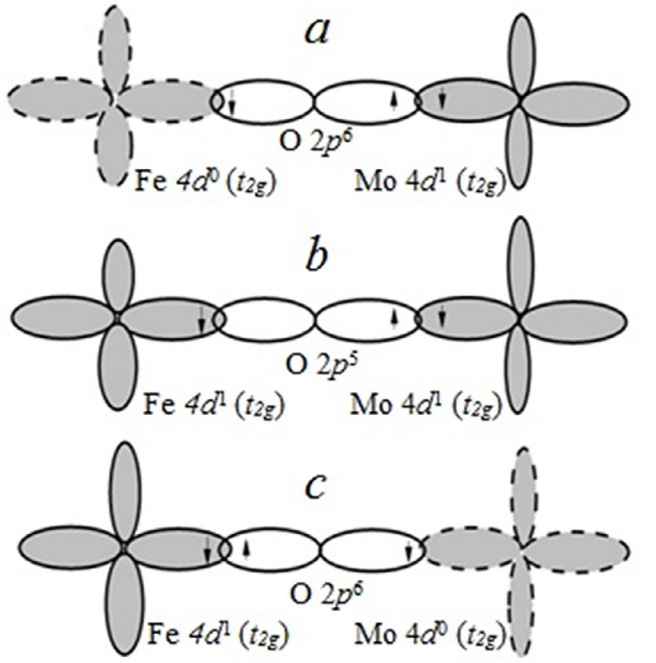

Fig. 5. Schematic image of the double exchange mechanism in the Sr_2FeMoO_{6-x} compound, where unfilled electron shells are indicated by the dashed line. a) Ground state; b) excited, metastable state; c) ground state.

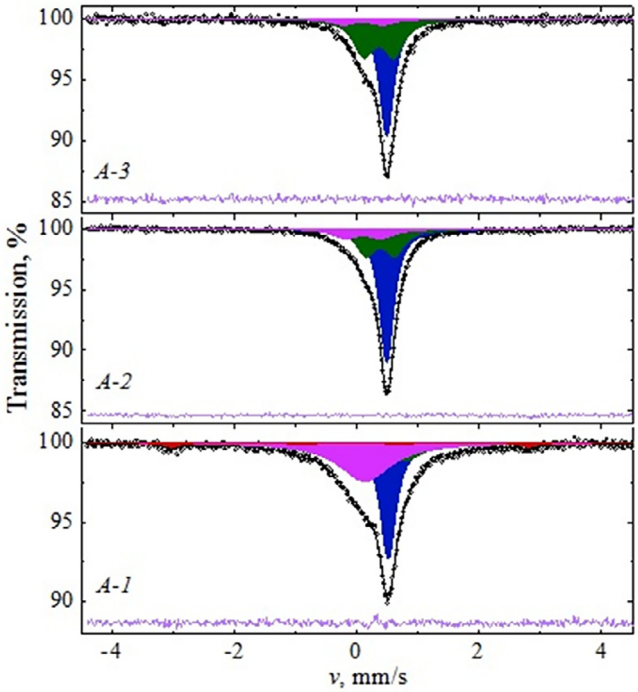

Fig. 6. Mössbauer spectra of the Sr_2FeMoO_{6-x} samples measured at 473 K (blue singlet is Fe^{3+} in the ordered clusters; green doublet is Fe^{3+} in the disordered clusters; purple doublet is Fe^{3+} in the defect clusters; red doublet is the metallic Fe). (For interpretation of the references to colour in this figure legend, the reader is referred to the web version of this article.)

of at least one more exchange interaction mechanism in the Sr_2FeMoO_{6-x}. Therefore, it is not quite correct to assume that the exchange interactions mechanism is realized only according to the Fe^{3+}–O–Mo^{5+} scheme. Moreover, a number of authors indicate the possibility of a realization of various exchange interaction mechanisms in the strontium ferromolybdate. In this way, it is pointed out in the paper [29], that the superexchange interaction between the ordered magnetic moments can realize the ferromagnetic magnetization of the samples. Tovar *et al.* [34] have admitted that the exchange interaction is realized through the free spin-polarized electrons, according to the Ruderman – Kittel – Kasuya – Yosida (RKKY) theory [29,31]. We are intent to support this assumption, as well, since according to the RKKY theory an increase of the free charge carriers leads to the rise of the density of states on the Fermi level, and, correspondingly, to the increase of the exchange interactions density and the rise of the Curie temperature at the increase of *P*, as we have observed in the present study. The Mössbauer spectroscopy data indicates an influence of the concentration of the spin-polarized charge carriers on the Fermi level on the magnetic properties of the compound.

It has been found in the process of a consideration of the Mössbauer spectra, measured in the paramagnetic phase at temperature 473 K, i.e. higher than the Curie temperature, that the Mössbauer spectrum of the *A*-1, *A*-2 and *A*-3 samples is successfully approximated as a superposition of three components (one S_1 singlet, two D1 and D2 doublets) (Fig. 6). Moreover, the S4 sextet lines are observed for the *A*-1 sample. This sextet was observed at low temperature (14 K), which corresponds to the iron clusters with the state close to the metallic one. The absence of S4 sextet lines on the spectra of other samples indicate the rise of magnetic inhomogeneity with an increase of the degree of the Fe/Mo cations superstructural ordering and the oxygen nonstoichiometry.

A singlet component on the Mössbauer spectra of the Sr_2FeMoO_{6-x} compound at 473 K corresponds to the $Fe^{2+/3+}$ ions in the areas ordered by the Fe/Mo cations, and the D1 doublet relates to the paramagnetic state of Fe ions in disordered areas (Table 3). Consequently, both ferrimagnetism and paramagnetism can coexist in the samples at a temperature close to T_C. Similar spectra, consisting of a singlet and a doublet, are observed for the $PbFe_{1/2}Sb_{1/2}O_3$ samples and solid solution on their base, having the cation ordering [35,37]. The D3 doublet with the minimal isomer shift corresponds to the Fe^{3+} with coordination number in the range 4–5 (Table 3). With a decrease of the ordering degree, the structural inhomogeneity rises in the samples, which leads to the increase of the width of the Mössbauer spectra component lines. For the same reason, the quadrupole splitting of the D2 and D3 doublets increases. The line broadening in the spectra of *A*-1 sample leads to a weak resolution of the quadrupole splitting lines depending on the local symmetry of electrical charge, and a zero quadrupole splitting takes place of the D3 doublet. This indicates the presence of various defects, whose concentration is larger than in the *A*-2 and *A*-3 samples, and promoting the increase of magnetic inhomogeneity in the *A*-1 sample.

For the investigation of the influence of the Fe/Mo cations superstructural ordering and oxygen nonstoichiometry on the magnetic phase transition temperature (T_C), temperature scanning technique has been implemented. Its essence is in a determination of the intensity of the Mössbauer spectra at the gradual decrease of temperature, where not the entire spectrum is measured, but fragments of spectrum are measured in the maximum of the resonance absorption for the paramagnetic phase (v = 0–1.2 mm/s) and in the absence of the resonance absorption (v = 12 mm/s). Difference of impulses in the indicated fragments corresponds to the maximum of the Mössbauer spectra lines intensity. At the magnetic phase transition the Mössbauer spectrum experience the Zeeman splitting, accompanied by a considerable decrease of the intensity of the lines, corresponding to the spectrum in the paramagnetic phase. Therefore, one can determine the magnetic phase transition temperature by the declination of the temperature dependence of the Mössbauer spectra lines intensity. This method was used for the investigations of the behavior of magnetic phase transitions temperatures in $AFe_{1/2}B_{1/2}O_3$ compounds (A = Ba, Ca, Pb, B-Nb,Ta, Sb), as well as in the solid solutions on their base [35–38]. The obtained results are in a good agreement with the data from the magnetic susceptibility measurements [39,40].

The the temperature scanning technique has been applied for a

Table 3
The Mössbauer spectra parameters of the Sr_2FeMoO_{6-x} samples, measured at 473 K.

Sample	Component	δ ± 0.01, mm/s	ε/Δ ± 0.01, mm/s	H ± 1, kOe	A ± 1, %	G ± 0.01, mm/s	χ^2
A-3	Singlet	0.47			51	0.29	1.031
	D2	0.36	0.49		42	0.41	
	D3	0.10	0.65		7	0.43	
A-2	Singlet	0.49			58	0.29	1.03
	D2	0.38	0.47		27	0.38	
	D3	0.10	0.60		13	0.50	
A-1	Singlet	0.51			34		1.121
	D2	0.38	0.79		21	0.71	
	D3	0.13	0		37	1.04	
	S4	−0.08	0.03	312	8	0.32	

where δ is the isomer shift; ε is the quadrupole shift; Δ is the quadrupole splitting; H is the hyperfine magnetic field on the ^{57}Fe nuclei; A is the area of the spectrum components; G is the width of the lines; χ^2 is the Pearson criterion

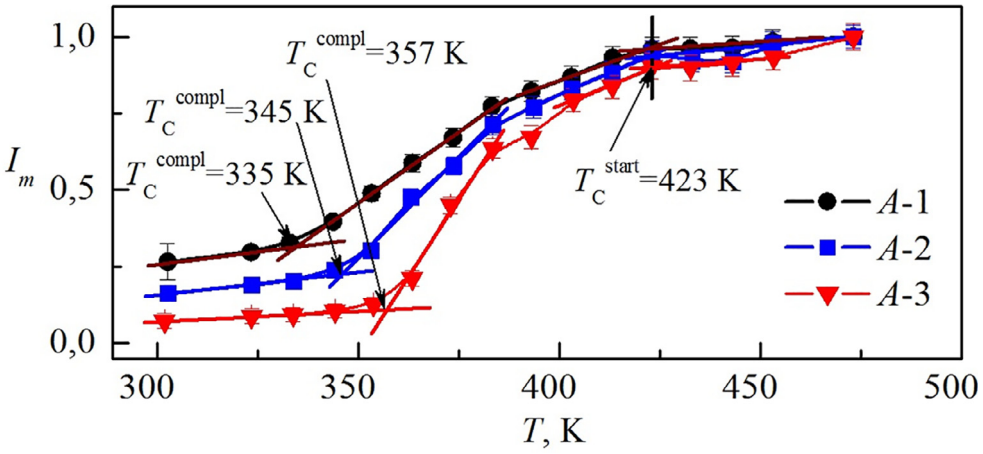

Fig. 7. Dependences of the intensity of the Mössbauer spectra paramagnetic lines of the Sr_2FeMoO_{6-x} samples, normalized on their values at 473 K.

determination of the temperature range of the magnetic phase transition. Temperature dependences of the intensity of paramagnetic lines (I_m) of the Mössbauer spectra, normalized on their values at 473 K are presented in Fig. 7.

The most intensive decline of the $I_m(T)$ dependences for all the Sr_2FeMoO_{6-x} samples is observed in the temperature range from 423 to 330 K. It is important to note, that at the transition to the ferrimagnetic phase the I_m value does not drop to zero, but it remains a finite value (Fig. 7). This is caused not only by the presence of magnetically-disordered (paramagnetic) inclusions at low temperatures, but also by the input of the sextet components in the velocity range 0–1.2 mm/s. As it has been determined the most intensive decline of the Mössbauer spectra paramagnetic lines, I_m is increasing with a rise of the Fe/Mo cations superstructural ordering. This indicates a decrease of the fraction of regions being disordered by the cations (Fig. 7).

As it has been mentioned before, a transition from the paramagnetic to the ferrimagnetic state is blurred. The point of the start (T_C^{start}) of the intensive decline of the $I_m(T)$ seems to be almost the same (≈423 K) for all the samples. This value is close to those determined by the temperature dependence of the magnetization (Fig. 2). The type of the $I_m(T)$ dependence makes it also possible to estimate the temperature of completion of the transition from the paramagnetic to the ferrimagnetic state T_C^{compl} and, correspondingly, possible to estimate the width of the transition blurring, which was difficult to realize from the temperature dependence of the magnetization. The T_C^{compl} values at cooling, estimated from the $I_m(T)$ behavior, are ≈335, ≈345 and ≈357 K, for the *A*-1, *A*-2 and *A*-3 samples, respectively. The width of the region of the blurring of the transition from the paramagnetic to the ferrimagnetic state, estimated by the $I_m(T)$ dependence, is ≈88, ≈78 and ≈66 K for the *A*-1, *A*-2 and *A*-3 samples, respectively. It is observed that the transition blurring increases with a decrease of *P*, at least fractionary, which could be caused by the increase of the anti-structural defects concentration.

It is well known, that the spin-polarization dynamics and the magnetic phase transition from the ferrimagnetic state to the paramagnetic one depends on the strength of the exchange interactions, as the T_C value in the AB′B″O_3 compounds depends on the Fe–O–Fe chains concentration [41]. At the increase of B-sublattice cations ordering degree, the number of Fe–O–Fe chains decreases, which leads to the lowering of the T_C value [37]. Probably, magnetic ordering in the studied samples is determined not only by the indirect cation-anion-cation exchange interaction, but the interaction through the conduction electrons, as well.

According to the Mössbauer spectroscopy investigations results, a fraction of the S1 sextet is increasing at the decrease of the anti-structural defects concentration with the increase of the oxygen vacancies in the *A*-1, *A*-2 and *A*-3 samples. This leads to a decrease of the Fe^{3+} cations concentration and the increase of the number of iron cations with the mixed valency $Fe^{3+/2+}$ being close to 2+. This is caused by the redistribution of electronic density together with a change of the electron configuration of the part of iron and molybdenum ions according to the scheme $Fe^{3+}(3d^5) + e \rightarrow Fe^{2+}(3d^6)$, $Mo^{5+}(4d^1) - e \rightarrow Mo^{6+}(4d^0)$. In this case, a part of the iron and molybdenum cations are passing to a more low-spin state, which in its turn increases the population degree of the $3d^6$ orbitals of the iron cations with electronic configurations $\{t_{2g\uparrow\downarrow\uparrow\uparrow}^4 e_{g\uparrow\uparrow}^2, S = 2\}$ and decreases the population of $4d^0$ molybdenum cations with electronic configurations $\{t_{2g}^0, S = 0\}$ (Fig. 8).

An increase of the $Fe^{2+}(3d^6)$ and $Mo^{6+}(4d^0)$ cations number

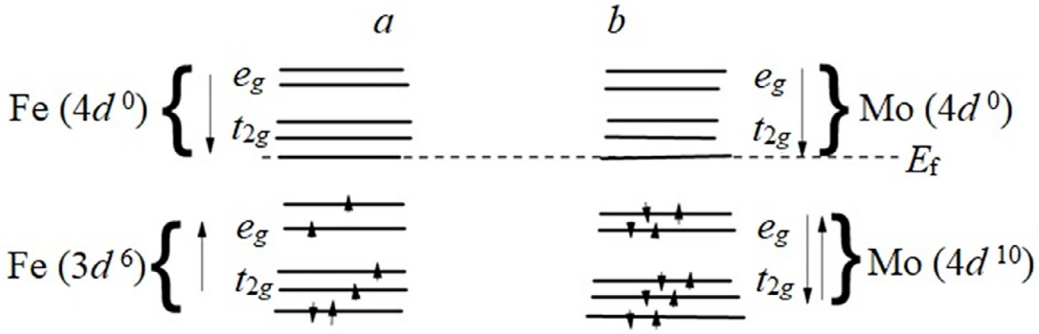

Fig. 8. Schematic image of the electrons distribution on the energy levels of iron ($Fe^{2+}(3d^6)$) and molybdenum ($Mo^{6+}(4d^0)$) in the Sr_2FeMoO_{6-x} compound at the presence of the antistructural defects. The Fermi level position is indicated by the dashed line. (a) Energy levels of iron; (b) energy levels of molybdenum.

promotes a partitioning of the long-chain ordering of the Fe^{3+}–O^{2-}–Mo^{5+} type and a decrease of the density of the free spin-polarized charge carriers on the Fermi level, and correspondingly, a decrease of the density of the exchange interactions and the Curie temperature, as we have observed earlier. Previous works [42–44] indicate a dependence of the Curie temperature on the bulk density of the exchange coupling, as well. Being based on the fact that the $Mo^{6+}(4d^0)$ diamagnetic cation does not take part in the exchange coupling, and only negative exchange couplings are possible between the $Fe^{2+}(3d^6)$ ions having smaller magnetic moment than the $Fe^{3+}(3d^5)$ ions, it is considered that the $Fe^{2+}(3d^6)$ ions are forming the antiferromagnetic ordering of magnetic moments. A similar situation with the negative exchange integral $J < 0$ has been observed in the double perovskites (Sr_2BMoO_6, where B = Ni, Co) with the substitution of iron and the presence of $Mo^{6+}(4d^0)$ in the molybdenum sublattice [43,45].

4. Conclusions

The single-phase Sr_2FeMoO_{6-x} polycrystalline samples with different oxygen content $(6-x)$ and various degrees of superstructural ordering of Fe/Mo cations (P) were obtained by the solid-phase method from the $SrFeO_{2.52}$ and $SrMoO_4$ precursors.

It has been determined as a result of the investigations of the influence of oxygen nonstoichiometry and the Fe/Mo cations superstructural ordering on magnetic properties of the Sr_2FeMoO_{6-x} compound, that with the rise of P and decrease of the oxygen index from $6-x = 5.99$ to 5.94, the magnetization values $M(T)$ increase in the temperature range 77–600 K.

It has been shown, that a monotonic decrease of T_C with a lowering of the P value is correlated also with an increase of the resistivity of the investigated samples, and correspondingly, with the drop of the concentration of the free charge carriers on the Fermi level. Our observation indicates an important role of the delocalized charge carriers, which agrees with the RKKY theory.

For all samples, it was found that with an increase in oxygen nonstoichiometry, the degree of superstructural ordering of Fe/Mo cations and, accordingly, the volume fraction of defect-free regions increases. The Mössbauer spectroscopy investigations results indicate this as well. These data confirm the increase of the S1 sextet area, corresponding to the $Fe^{2+/3+}$ ions in the highly-ordered regions and the decrease of the area of the S2 sextet, related to the disordered regions.

Temperatures of the starting (T_c^{start}) and completion (T_c^{compl}) of the transition from the paramagnetic to the ferrimagnetic state are analyzed together with the width of the transition blurring based on the type of the $I_m(T)$ dependence. The T_c^{compl} values at cooling are ≈335, ≈345 and ≈357 K, for the A-1, A-2 and A-3 samples, respectively. Values for the width of the blurring region for the transition from the paramagnetic to the ferrimagnetic state is ≈88, ≈78 and ≈66 K for the A-1, A-2 and A-3 samples, respectively. The transition blurring width increases with a decrease of P, at least fractionary, which could be caused by the increase of the anti-structural defects concentration.

CRediT authorship contribution statement

Nikolay Kalanda: Conceptualization. **Marta Yarmolich:** Writing - original draft. **Alexander Petrov:** Writing - original draft. **Igor Raevski:** Data curation. **Stanislav Kubrin:** Methodology. **Svetlana Raevskaya:** Data curation. **Ivan Bobrikov:** Methodology. **Andrei Lazavenka:** Data curation. **Dong-Hyun Kim:** Writing - review & editing.

Declaration of Competing Interest

The authors declare that they have no known competing financial interests or personal relationships that could have appeared to influence the work reported in this paper.

Acknowledgments

The authors acknowledge the support of the work in frames of the European project H2020-MSCA-RISE-2017-778308 – SPINMULTIFILM. The reported research was supported by the Russian Fundamental Research Foundation (project No. 19-32-50048 mol_nr).

References

[1] J. Cibert, J.-F. Bobo, U. Lüders, Development of new materials for spintronics, CR Phys. 6 (2005) 977–996, https://doi.org/10.1016/j.crhy.2005.10.008.
[2] N. Kalanda, D.-H. Kim, S. Demyanov, S.-C. Yu, M. Yarmolich, A. Petrov, S.K. Oh, Sr_2FeMoO_6 nanosized compound with dielectric sheaths for magnetically sensitive spintronic devices, Curr. Appl. Phys. 18 (2018) 27–33, https://doi.org/10.1016/j.cap.2017.10.018.
[3] L.V. Kovalev, M.V. Yarmolich, M.L. Petrova, J. Ustarroz, H. Terryn, N.A. Kalanda, M.L. Zheludkevich, Double perovskite Sr_2FeMoO_6 films prepared by electrophoretic deposition, ACS Appl. Mater. Interfaces 6 (2014) 19201–19206, https://doi.org/10.1021/am5052125.
[4] D. Serrate, J.M. De Teresa, M.R. Ibarra, Double perovskites with ferromagnetism above room temperature, J. Phys. Condens. Matter. 19 (2007), https://doi.org/10.1088/0953-8984/19/2/023201.
[5] N. Kalanda, S. Demyanov, W. Masselink, A. Mogilatenko, M. Chashnikova, N. Sobolev, O. Fedosenko, Interplay between phase formation mechanisms and magnetism in the Sr_2FeMoO_6 metal-oxide compound, Cryst. Res. Technol. 46 (2011) 463–469, https://doi.org/10.1002/crat.201000213.
[6] N.A. Kalanda, S.E. Demyanov, A.V. Petrov, D.V. Karpinsky, M.V. Yarmolich, S.K. Oh, S.C. Yu, D.-H. Kim, Interrelation between the structural, magnetic and magnetoresistive properties of double-perovskite $Sr_2FeMoO_{6-\delta}$ thin films, J. Electron. Mater. 45 (2016) 3466–3742, https://doi.org/10.1007/s11664-016-4478-5.
[7] K.-I. Kobayashi, T. Kimura, H. Sawada, K. Terakura, Y. Tokura, Room-temperature magnetoresistance in an oxide material with an ordered double-perovskite structure, Nature 395 (1998) 677–680, https://doi.org/10.1038/27167.
[8] R. Allub, O. Navarro, M. Avignon, B. Alascio, Efect of disorder on the electronic structure of the double perovskite Sr_2FeMoO_6, Phys. B Condens. Matter. 320 (2002) 13–17, https://doi.org/10.1016/S0921-4526(02)00608-7.
[9] A. Sharma, J.L. MacManus-Driscoll, W. Branford, Y. Bugoslavsky, L.F. Cohen,

J. Rager, Phase stability and optimum oxygenation conditions for Sr_2FeMoO_6 formation, Appl. Phys. Lett. 87 (2005) 112505, https://doi.org/10.1063/1.2048810.
[10] Z. Klencsár, Z. Németh, A. Vértes, I. Kotsis, M. Nagy, Á. Cziráki, C. Ulhaq-Bouillet, V. Pierron-Bohnes, K. Vad, S. Mészáros, J. Hakl, The effect of cation disorder on the structure of Sr_2FeMoO_6 double perovskite, J. Magn. Magn. Mater. 281 (2004) 115–123, https://doi.org/10.1016/j.jmmm.2004.04.097.
[11] D.D. Sarma, P. Mahadevan, T. Saha-Dasgupta, S. Ray, A. Kumar, Electronic structure of Sr_2FeMoO_6, Phys. Rev. Lett. 85 (2000) 2549, https://doi.org/10.1103/PhysRevLett. 85.2549.
[12] Y. Matsuda, M. Karppinen, Y. Yamazaki, H. Yamauchi, Oxygen-vacancy concentration in $A_2MgMoO_{6-\delta}$ double-perovskite oxides, J. Solid State Chem. 182 (2009) 1713–1716, https://doi.org/10.1016/j.jssc.2009.04.016.
[13] D. Niebieskikwiat, A. Caneiro, R.D. Sánchez, J. Fontcuberta, Oxygen-induced grain boundary effects on magnetotransport properties of $Sr_2FeMoO_{6+\delta}$, Phys. Rev. B 64 (2001) 180406, https://doi.org/10.1103/PhysRevB.64.180406.
[14] J. MacManus-Driscoll, A. Sharma, Y. Bugoslavsky, W. Branford, L.F. Cohen, M. Wei, Reversible low-field magnetoresistance in $Sr_2Fe_{2-x}Mo_xO_{6-\delta}$ by oxygen cycling and the role of excess Mo (x > 1) in grain-boundary regions, Adv. Mater. 18 (2006) 900–904, https://doi.org/10.1002/adma.200501277.
[15] M.E. Matsnev, V.S. Rusakov, SpectrRelax: an application for Mössbauer spectra modeling and fitting, AIP Conf. Proc. 1489 (2012) 178–185, https://doi.org/10.1063/1.4759488.
[16] N.A. Kalanda, V.A. Turchenko, D.V. Karpinsky, S.E. Demyanov, M.V. Yarmolich, M. Balasiou, N. Lupu, S.I. Tyutyunnikov, N.A. Sobolev, The role of the Fe/Mo cations ordering degree and oxygen non-stoichiometry on the formation of the crystalline and magnetic structure of $Sr_2FeMoO_{6-\delta}$, Phys. Status Solidi B 256 (2019) 1800278, https://doi.org/10.1002/pssb.201800278.
[17] F. Menil, Systematic trends of the 57Fe Mössbauer isomer shifts in (FeOn) and (FeFn) polyhedra. Evidence of a new correlation between the isomer shift and the inductive effect of the competing bond T-X (→ Fe) (where X is O or F and T any element with a formal positive charge), J. Phys. Chem. Solids 46 (7) (1985) 763–789, https://doi.org/10.1016/0022-3697(85)90001-0.
[18] J.G. Stevens, A.M. Khasanov, J.W. Miller, H. Pollak, Z. Li, Mössbauer Mineral Handbook, The University of North Carolina at Asheville Mössbauer Effect Data Center, USA, 2002.
[19] I.P. Raevski, S.P. Kubrin, S.I. Raevskaya, D.A. Sarychev, S.A. Prosandeev, M.A. Malitskaya, Magnetic properties of $PbFe_{1/2}Nb_{1/2}O_3$: Mössbauer spectroscopy and first-principles calculations, Phys. Rev. B 85 (2012), https://doi.org/10.1103/PhysRevB.85.224412 224412.
[20] V.S. Rusakov, V.S. Pokatilov, A.S. Sigov, M.E. Matsnev, T.V. Gubaidulina, Diagnostics of a spatial spin-modulated structure using nuclear magnetic resonance and Mössbauer spectroscopy, JETP Lett. 100 (2014) 463–469, https://doi.org/10.1134/S0021364014190102.
[21] J.M. Greneche, M. Venkatesan, R. Suryanarayanan, J.M.D. Coey, Mössbauer spectrometry of A_2FeMoO_6 (A = Ca, Sr, Ba): search for antiphase domains, Phys. Rev. B 63 (2001) 174403, https://doi.org/10.1103/PhysRevB.63.174403.
[22] O. Chmaissem, R. Kruk, B. Dabrowski, D.E. Brown, X. Xiong, S. Kolesnik, J.D. Jorgensen, C.W. Kimball, Structural phase transition and the electronic and magnetic properties of Sr_2FeMoO_6, Phys. Rev. B 62 (2000) 14197, https://doi.org/10.1103/PhysRevB.62.14197.
[23] J. Linden, M. Karppinen, T. Shimada, Y. Yasukawa, H. Yamauchi, Observation of antiphase boundaries in Sr_2FeMoO_6, Phys. Rev. B 68 (2003) 174415, https://doi.org/10.1103/PhysRevB.68.174415.
[24] A.V. Pavlenko, S.P. Kubrin, A.T. Kozakov, L.A. Shilkina, L.A. Reznichenko, A.V. Nikolskii, V.V. Stashenko, Y.V. Rusalev, K.S. Petrosyan, Phase transitions, dielectric, magnetic properties and valence of ions in $AFe_{2/3}W_{1/3}O_{3\pm\sigma}$ (A = Ba, Sr) multiferroic ceramics, J. Alloys Compd. 740 (2018) 1037–1045, https://doi.org/10.1016/j.jallcom.2018.01.060.
[25] N.A. Kalanda, V.M. Garamus, M.V. Avdeev, M.L. Zheludkevich, M.V. Yarmolich, M.V. Serdechnova, D.C.F. Wieland, A.V. Petrov, A.L. Zhaludkevich, N.A. Sobolev, Small-angle neutron scattering and magnetically heterogeneous state in $Sr_2FeMoO_{6-\delta}$, Phys. Status Solidi B 256 (2019) 1800428, https://doi.org/10.1002/pssb.201800428.
[26] P. Kapitza, The study of the specific resistance of bismuth crystals and its change in strong magnetic fields and some allied problems, Proc. Roy. Soc. A 119 (1928) 358–443, https://doi.org/10.1098/rspa.1928.0103.
[27] E.N. Adams, T.D. Holstein, Quantum theory of transverse galvanomagnetic phenomena, J. Phys. Chem. Sol. 10 (1959) 254–276, https://doi.org/10.1016/0022-3697(59)90002-2.
[28] J.B. Goodenough, Localized to Itinerant Electronic Transition in Perovskite Oxides, Springer-Verlag, Berlin, 2001.
[29] M. Besse, V. Cros, A. Barthelemy, H. Jaffres, J. Vogel, F. Petroff, A. Mirone, A. Tagliaferri, P. Bencok, P. Decorse, P. Berthet, Z. Szotek, W.M. Temmerman, S.S. Dhesi, N.B. Brookes, A. Rogalev, A. Fert, Experimental evidence of the ferrimagnetic ground state of Sr_2FeMoO_6 probed by X-ray magnetic circular dichroism, Europhys. Lett. 60 (2002) 608–614, https://doi.org/10.1209/epl/i2002-00262-4.
[30] J. Lindén, T. Yamamoto, M. Karppinen, H. Yamauchi, Evidence for valence fluctuation of Fe in Sr_2FeMoO_{6-w} double perovskite, Appl. Phys. Lett. 76 (2000) 2925–2927, https://doi.org/10.1063/1.126518.
[31] L. dos Santos-Gomez, L. Leon-Reina, J.M. Porras-Vazquez, E.R. Losilla, D. Marrero-Lopez, Chemical stability and compatibility of double perovskite anode materials for SOFCs, Solid State Ionics 239 (2013) 1–7, https://doi.org/10.1016/j.ssi.2013.03.005.
[32] M.C. Viola, M.J. Martinez-Lope, J.A. Alonso, P. Velasco, J.L. Martinez, J.C. Pedregosa, R.E. Carbonio, M.T. Fernandez-Diaz, Induction of colossal magnetoresistance in the double perovskite Sr_2CoMoO_6, Chem. Mater. 14 (2002) 812–818, https://doi.org/10.1021/cm011186j.
[33] C. Ritter, M.R. Ibarra, L. Morellon, J. Blasco, J. Garcia, J.M. De Teresa, Structural and magnetic properties of double perovskites AA'FeMoO6 (AA' = Ba2, BaSr, Sr2 and Ca2), J. Phys. Condens. Matter. 12 (2000) 8295–8308, https://doi.org/10.1088/0953-8984/12/38/306.
[34] M. Tovar, M.T. Causa, A. Butera, J. Navarro, B. Martinez, J. Fontcuberta, M.C.G. Passeggi, Evidence of strong antiferromagnetic coupling between localized and itinerant electrons in ferromagnetic Sr_2FeMoO_6, 024409, Phys. Rev. B. 66 (2002), https://doi.org/10.1103/PhysRevB.66.024409.
[35] I.P. Raevski, A.V. Pushkarev, S.I. Raevskaya, N.M. Olekhnovich YuV, S.P. Radyush, H. Kubrin, C.-C. Chen, D.A. Chou, V.V. Sarychev Titov, M.A. Malitskaya, Structural, dielectric and Mössbauer studies of $PbFe_{0.5}Sb_{0.5}O_3$ ceramics with differing degree of compositional ordering, Ferroelectrics 501 (2016) 154–164, https://doi.org/10.1080/00150193.2016.1204196.
[36] I.P. Raevski, S.P. Kubrin, S.I. Raevskaya, V.V. Titov, S.A. Prosandeev, D.A. Sarychev, M.A. Malitskaya, V.V. Stashenko, I.N. Zakharchenko, Studies of ferroelectric and magnetic phase transitions in $Pb_{1-x}A_xFe_{1/2}Nb_{1/2}O_3$ (A-Ca, Ba) solid solutions, Ferroelectrics 398 (2010) 16–25, https://doi.org/10.1080/00150193.2010.489807.
[37] I.P. Raevski, N.M. Olekhnovich, A.V. Pushkarev, Y.V. Radyush, S.P. Kubrin, S.I. Raevskaya, M.A. Malitskaya, V.V. Titov, V.V. Stashenko, Mössbauer studies of $PbFe_{0.5}Nb_{0.5}O_3$ – $PbFe_{0.5}Sb_{0.5}O_3$ multiferroic solid solutions, Ferroelectrics 444 (2013) 47–52, https://doi.org/10.1080/00150193.2013.785914.
[38] A.A. Gusev, S.I. Raevskaya, V.V. Titov, E.G. Avvakumov, V.P. Isupov, I.P. Raevski, H. Chen, C.-C. Chou, S.P. Kubrin, S.V. Titov, M.A. Malitskaya, A.V. Blazhevich, D.A. Sarychev, V.V. Stashenko, S.I. Shevtsova, Dielectric and Mossbauer studies of $Pb(Fe_{1/2}Ta_{1/2})O_3$ multiferroic ceramics sintered from mechanoactivated powders, Ferroelectrics 475 (2015) 41–51, https://doi.org/10.1080/00150193.2015.995007.
[39] V.V. Laguta, V.A. Stephanovich, M. Savinov, M. Marysko, R.O. Kuzian, N.M. Olekhnovich, A.V. Pushkarev, Yu.V. Radyush, I.P. Raevski, S.I. Raevskaya, S.A. Prosandeev, Superspin glass phase and hierarchy of interactions in multiferroic $PbFe_{1/2}Sb_{1/2}O_3$: an analog of ferroelectric relaxors? New J. Phys. 16 (2014), https://doi.org/10.1088/1367-2630/16/11/113041 113041.
[40] M. Marysko, V. Laguta, I.P. Raevski, R.O. Kuzian, N.M. Olekhnovich, A.V. Pushkarev, Yu.V. Radyush, S.I. Raevskaya, V.V. Titov, S.P. Kubrin, Magnetic susceptibility of multiferroics and chemical ordering, 056409, AIP Adv. 7 (2017), https://doi.org/10.1063/1.4973601.
[41] J.B. Goodenough, Magnetism and Chemical Bond, Interscience Publishers (1963).
[42] M.K. Chung, P.J. Huang, W.H. Li, C.C. Yang, T.S. Chan, R.S. Liu, S.Y. Wu, J.W. Lynn, Crystalline and magnetic structures of Sr_2FeMoO_6 double perovskites, Physica B 385–386 (2006) 418–420, https://doi.org/10.1016/j.physb.2006.05.140.
[43] J.-S. Kang, J.H. Kim, A. Sekiyama, S. Kasai, S. Suga, S.W. Han, K.H. Kim, T. Muro, Y. Saitoh, C. Hwang, C.G. Olson, B.J. Park, B.W. Lee, J.H. Shim, J.H. Park, B.I. Min, Bulk-sensitive photoemission spectroscopy of A_2FeMoO_6 double perovskites (A = Sr, Ba), 113105, Phys. Rev. B. 66 (2002), https://doi.org/10.1103/PhysRevB.66.113105.
[44] T. Suominen, J. Raittila, T. Salminen, K. Schlesier, J. Linden, P. Paturi, Magnetic properties of fine SFMO particles: superparamagnetism, J. Magn. Magn. Mater. 309 (2007) 278–284, https://doi.org/10.1016/j.jmmm.2006.07.016.
[45] J. Rager, M. Zipperle, A. Sharma, J.L. MacManus-Driscoll, Oxygen stoichiometry in Sr_2FeMoO_6, the determination of Fe and Mo valence states, and the chemical phase diagram of SrO – Fe_3O_4 – MoO_3, J. Am. Ceram. Soc. 87 (2004) 1330–1335, https://doi.org/10.1111/j.1151-2916.2004.tb07730.x.